Available online at www.sciencedirect.com
ScienceDirect
ELSEVIER
International Journal of Thermal Sciences 46 (2007) 1191–1202
International Journal of Thermal Sciences
www.elsevier.com/locate/ijts

Multi-objective design optimization of topology and performance of branching networks of cooling passages ☆

Maickel Gonzalez [a,1], Nenad Jelisavcic [a,2], Ramon J. Moral [a,3], Debasis Sahoo [a,4], George S. Dulikravich [a,*,5], Thomas J. Martin [b,6]

[a] *Department of Mechanical and Materials Engineering, Multidisciplinary Analysis, Inverse Design and Robust Optimization Center (MAIDROC), Florida International University, 10555 West Flagler Street, Miami, FL 33174, USA*

[b] *Pratt & Whitney Engine Company, Turbine Discipline Engineering & Optimization Group, M/S 169-20, 400 Main Street, East Hartford, CT 06108, USA*

Received 1 August 2006; received in revised form 12 June 2007; accepted 12 June 2007

Available online 25 July 2007

Abstract

The objective of this study was to develop an automatic, self-sufficient, preliminary design algorithm for optimization of topologies of branching networks of internal cooling passages. Optimization with four levels of fractal branching channel networks was tested. The number of branches per level was optimized in order to minimize coolant mass flow rate, total pressure drop, and maximize total heat removed. The software package includes a random branches generator, a quasi 1-D thermo-fluid analysis code, and a multi-objective hybrid optimizer. The heat transfer/flow-field analysis software has been verified against a similar analysis code used by Pratt & Whitney Company. The hybrid multi-objective optimization code was verified against classical test cases involving multiple objectives. In this work the total number of Pareto-optimal designs was 100. After finding the Pareto optimized configurations, the user has to decide which optimized cooling network configuration is the best for the desired application. It was demonstrated that this can be accomplished by utilizing Pareto-optimal solutions to create a curve representing pumping power vs. total heat removed and by observing which designs provide favorable break-even energy transfer.

Keywords: Optimization; Branching micro-channels; Cooling; Thermal design; Heat exchangers

1. Introduction

A fractal branches generator program was created to obtain a network of fractal branching channels in a random fashion [1]. This program was written in the FORTRAN programming language and it allows having a different fractal branching geometry every time the program runs. The network consists of two possible scenarios. One is a diverging branching network, similar to the roots in a tree, and the other is a diverging–converging branching network, similar to the veins and arteries in the human body. In this work only the diverging fractal branching network was used for possible future applications involving film cooling from a large number of exit microchannels. Thus, each configuration was allowed to have one inlet and a random number of exits. The internal fluid flow properties through the branching geometry were solved with a quasi one-dimensional (1-D), finite element, compressible thermo-fluid flow network analysis program and the whole geometry of the system was

☆ This paper represents a revised version of the following paper: M.J. Gonzalez, R.J. Moral, T.J.M. Martin, D. Sahoo, G.S. Dulikravich, N. Jelisavcic, Multi-objective design optimization of topology and performance of branching networks of cooling passages, ASME paper ICNMM2006-96151, in: S. Kandlikar (Ed.), ASME Fourth International Conference on Nanochannels, Microchannels and Minichannels, University of Limerick, Limerick, Ireland, June 19–21, 2006.

* Corresponding author. Tel.: +1 (305) 348 7016; fax: +1 (305) 348 6007.
E-mail address: dulikrav@fiu.edu (G.S. Dulikravich).

[1] Graduate student. Currently certification engineer with B/E Aerospace, Florida.

[2] Graduate student. Currently chief engineer with Bio-Nucleonics, Inc., Miami, Florida.

[3] Graduate student.

[4] Graduate student. Currently with Infinite Cloud, LLC, New York City, New York.

[5] Professor and chairman, MME Department. Director of MAIDROC.

[6] Senior systems design engineer.

1290-0729/$ – see front matter
doi:10.1016/j.ijthermalsci.2007.06.010

Nomenclature

A_k	Cross-section area of a channel in segment k
C_p	Specific heat of coolant
d_k	Hydraulic diameter of a channel in segment k
D	Euclidean dimension
f	Friction coefficient
h_c	Heat transfer coefficient on internal surfaces
k	Branching level number
L_k	Length of a channel in segment k
L_m	Terminal channel length
L_{tot}	Total channel length
$\dot{m}$	Mass flow rate in a coolant passage
m	Total number of branching levels exclusive of 0th level
n	Number of branches into which a single channel splits
Pr	Prandtl number
P_t	Total pressure in coolant fluid system
ΔP_t	Total pressure drop
$\dot{Q}$	Total heat removed
St	Stanton number
Re_D	Reynolds number
$T_{t,c}$	Bulk total temperature of coolant
w	Average local coolant speed

Greek letters

β	Branching diameter ratio
γ	Branching length ratio
ε	Relative surface roughness of the cooling channel
μ	Coefficient of viscosity of the coolant
ρ	Density of coolant
τ_w	Wall shear stress

Subscripts

avg	Average
c	Coolant/channel surface
ref	Reference value
t	Total or absolute value

optimized. In the quasi 1-D, finite element, thermo-fluid flow network analysis program COOLNET [2–4], semi-empirical correlations were used to determine the coolant heat transfer coefficients, h_c, while the quasi one-dimensional momentum and enthalpy equations were solved for the total pressure losses and bulk coolant temperatures, $T_{t,c}$, of the coolant fluid. The heat transfer coefficients and bulk coolant temperatures were assumed to vary in the coolant flow direction.

The geometric properties of connecting elements such as cross-section areas, hydraulic diameters, and element lengths were calculated based on suggestions made by West et al. [5,6] for two-dimensional flow networks. Then, network connections were optimized by allowing the number of branching elements per node to vary from one to five in order to simultaneously achieve three design objectives: maximize the total amount of heat removed by the coolant fluid, minimize the coolant mass flow rate and minimize the total pressure drop of the coolant. This amounted to a total of three design objectives and 31 design variables (branching nodes at which the optimum number of emanating channels needs to be determined) for the case of a cooling network having four branching levels (Fig. 1).

A hybrid multi-objective optimization algorithm, [7], capable of dealing with several objective functions simultaneously in a Pareto front optimal sense, was used to perform the optimization process. The hybrid optimization algorithm includes multi-objective versions of three evolutionary optimization algorithms, these are: non-dominated sorting differential evolution (NSDE), [8], strength Pareto evolutionary algorithm (SPEA), [9], and a multi-objective particle swarm (MOPSO) algorithm based on particle swarm, [10]. An automatic switching algorithm was created [7] to switch among the three multi-objective optimization algorithms [11] during the optimization in order to avoid any stalling or meandering of successive Pareto front approximations.

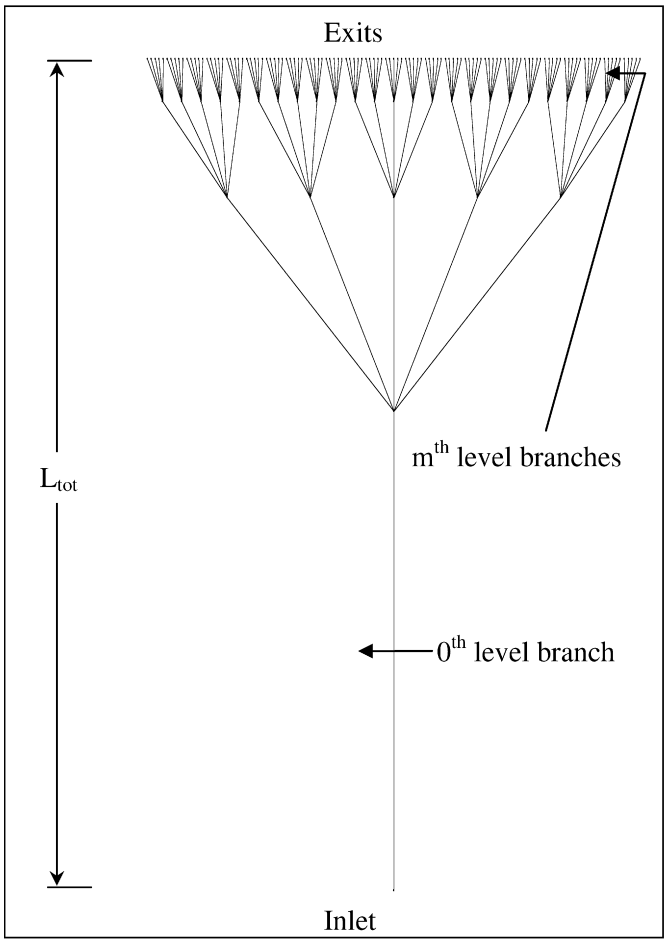

Fig. 1. Geometry of initial cooling configuration with 4 branching levels and 156 branches depicting direction of coolant flow, inlet and 125 exits.

2. Physical and mathematical model

The shape of the initial cooling passages is an internal network of fractal branching channels and is presented in Fig. 1. The cooling network was allowed to have an arbitrary number of inlet nodes and exit nodes, although in the examples considered in this work the network consists of one inlet and up to 125 possible exits. All nodes are evenly spaced across a maximum width of 0.03 m. In Fig. 1 the flow direction is shown to represent how the coolant fluid moves through the fractal branching network. Element properties like cross sectional areas, hydraulic diameters, and lengths were calculated using the assumed (non-optimal) ratio formulas of West et al. [5,6].

The computer program used to analyze the cooling properties of the initial configurations shown in Fig. 1 also can account for micro ribs, staggered and inline rows of pin fins and impingement holes, but these features were not used in this work [2–4,12].

The internally cooled object involves a network with many branches and various types of connections that could be easily developed by using the automatic branches generator with a variable number of connections between the nodes.

The Reynolds analogy provided a relationship between the wall shear stress and the heat transfer.

$$St = \frac{f/8}{1 + 12.7(Pr^{2/3} - 1)\sqrt{f/8}} \tag{1}$$

Here, the Stanton number, $St = h_c/\rho c_p w$, the Prandtl number, $Pr = \mu c_p/k$, and the friction factor, $f = 8\tau_w/\rho w^2$, were based on the bulk properties of the coolant fluid. The value of the friction factor was taken from the Moody diagram knowing the relative roughness ratio, ε/D_h, and the Reynolds number [13, pp. 230].

Each fluid element (a member of the cooling network which connects two nodes) can have different wall roughness, angle, length, cross-sectional area and geometry. Local hydrodynamic losses were computed in each fluid element based on the local value of the Reynolds number used in an explicit formula given by Haaland [14].

$$\frac{1}{\sqrt{f}} = -1.8\log\left[\frac{6.9}{Re_D} + \left(\frac{\varepsilon/D_h}{3.7}\right)^{1.11}\right] \tag{2}$$

The ejection static pressure can be either computed by a CFD or it can be specified as a design condition (in the case of a closed loop cooling systems). The resulting inlet coolant static pressure was a function of the coolant mass flow rate, the relative wall roughness, the inlet coolant air pressure, the material properties, coolant passage geometry, and the heat flux into the cooled object.

The scheme of Fig. 1 is used for calculation in this work and it is optimized to give the best cooling performance by allowing the number of branches developing from any single channel to vary from 1 to 5 while keeping all other element properties such as; channel lengths, cross-sectional areas, hydraulic diameter, and wall roughness fixed. For more general calculations this network can be developed with other geometries, with different arrangement of connections between the nodes, different number of nodes, different number of elements, etc.

In Fig. 1 each node is represented by the intersection where one or more lines join and each element is a line connecting two nodes. The coolant flow enters through the inlet and leaves through all the exits. The internal coolant network was subdivided into kk elements (fluid paths). Fluid elements were connected, as presented in Fig. 1, between nn nodes. The number of inlet and exit nodes, mm, was included in the total number of nodes, nn. Each fluid element has two nodal endpoints (inlet and exit). Internal nodes have at least one path entering it (source) and one or more paths leaving (sink). Nodes that have no sources, having one or more sink paths indicate a supply (inlet) path. Similarly, nodes connected to one or more sources, having no sink paths are called a dump (exit) path.

3. Creating the network geometry

Geometric information of the internal coolant passages was accomplished by using the fixed ratios found in the work of West et al. [5,6] for two-dimensional branching channel networks. These ratios give the branching diameter and lengths ratios

$$\beta = \frac{d_{k+1}}{d_k} = n^{-1/(D+1)} \tag{3}$$

$$\gamma = \frac{L_{k+1}}{L_k} = n^{-1/D} \tag{4}$$

The symbol γ represents the branching length ratio, β represents the branching diameter ratio, m indicates the total number of branching levels exclusive of 0th level which is the inlet of the branches, n represents the number of branches into which a single channel branches, D is the Euclidean dimension, d_k represents the hydraulic diameter of a channel in segment k, and L_k represents the length of a channel in segment k, where k is indexed from *zero* to m. Specifying a total channel length L_{tot} and using the relation

$$L_m = \frac{L_{\text{tot}}}{\sum_{i=0}^{m} \frac{1}{\gamma^i}} \tag{5}$$

to find the terminal channel length L_m, allows to calculate the length of all the branching levels by using Eq. (5). In a similar fashion all the hydraulic diameters are calculated using Eq. (4) given the hydraulic diameter of any branching level. These ratio formulas were originally derived for the assumed trees, not optimized trees [15], while most of the dendritic architectures in heat transfer today are optimized trees arising from constructal theory [16–19]. However, no mathematical formulations from the constructal theory were used in the present work which serves purely as proof of a concept for designing cooling networks having multiple objectives by using a multi-objective optimization algorithm. The branching angles were not taken into account in the current analysis nor in the optimization logic.

The random branches generator was initialized as shown in Fig. 1, to a maximum of five branching channels extending from each channel ($n = 5$), four branching levels ($m = 3$ when excluding the 0th level), for a two-dimensional object ($D = 2$) having total channel length $L_{\text{tot}} = 0.06$ meters and an inlet hydraulic diameter $d_{k=0} = 2.006 \times 10^{-3}$ meters.

Table 1
Geometry dimensions for four levels of branching channels shown in Fig. 1

k	A_k (m)	$d_{H,k}$ (m)	L_k (m)
0	1.504×10^{-4}	2.006×10^{-3}	3.455×10^{-2}
1	8.795×10^{-6}	1.173×10^{-3}	1.545×10^{-2}
2	5.144×10^{-6}	6.860×10^{-4}	6.910×10^{-3}
3	3.008×10^{-6}	4.012×10^{-4}	3.090×10^{-3}
		Total	6.000×10^{-2}

The fixed ratios formulas (Eqs. (3) and (4)) were used in this paper with a fixed value of γ. This results in a fixed length of each level of branching. This would lead to non-uniform distances between neighboring branching levels. However, we were interested in the case where all the branching nodes on the same branching level (that is, on a straight line) are at the same location measured along the main flow direction (see Fig. 1). It is these distances between the neighboring branching levels that were computed using the fixed ratios formulas (Eqs. (3) and (4)). Since these ratio formulas are not giving optimized values of channel diameters and their lengths, the lengths of all channels except for the central channel are definitely suboptimal in the example treated in this work.

Due to anticipated long computing time needed, in this particular work, our objective was not to optimize the length of each individual channel and its diameter and surface roughness. However, it could be a simple future extension of this work to use an optimization algorithm and these three quantities per each segment of each flow channel as additional design variables.

Table 1 (first two rows) illustrates the values to which channels in each level were initialized using the diameter and length ratios calculated before. Other initialization parameters were the interior wall roughness and the wall surface temperature for each channel. These initial values were 0.3175×10^{-3} m and 1025 K, respectively. In this work, the interior wall roughness was kept constant for all the elements in the fractal branching network. The working fluid was air with its temperature-dependent physical properties. The boundary conditions at the inlet were a total pressure of 1706.6 kPa and a total temperature of 893.37 K. The boundary conditions at the exits were a static ambient pressure of 752.89 kPa and a static temperature of 1366.4 K. The local average coolant speeds, pressures and temperatures were then calculated by iteratively satisfying a system of local mass conservations and extended Bernoulli's equations involving heat transfer, enthalpy changes and viscous losses [2–4,12]. Surfaces of all the channels were kept isothermal throughout the optimization process with a steady cold stream feeding through a single inlet and leaving as warm shower through a canopy of exit channels.

4. Optimization process

The hybrid multi-objective optimizer combined with the fractal branches generator and the quasi 1-D flow field/heat transfer analysis is used to optimize the internal passage geometry for optimum flow properties and geometry. Program OBJ is written as the connection between the branches generator, the quasi 1-D analysis code and the hybrid multi-objective optimizer. Program OBJ, which is called by the optimization algorithm performs the following tasks:

- Reads branching generator's initial input file.
- Reads optimizer's output file.
- Writes new branches generator's input file based on optimizer's output file.
- Runs the branches generator program.
- Branches generator writes an input file for the quasi 1-D flow-field analysis code.
- Runs quasi 1-D flow-field analysis code using input given by branches generator.
- Reads total number of elements from the quasi 1-D thermo-fluid analysis input file.
- Reads output file from the quasi 1-D thermo-fluid analysis code.
- Calculates objectives.
- Writes input file for optimizer.

With the last step, the optimizer makes decisions and the process repeats in a loop until the desired number of function evaluations is reached.

The design variables in this research are the number of branching channels allowed to propagate from a single channel. For all the channels the number of developing branching channels was allowed to vary from 1 to 5. The simultaneous objectives were as follows:

- Total heat removed (to be maximized)—is the heat, which the coolant absorbs from the walls per unit time.
- Total pressure drop (to be minimized)—is the total pressure difference between inlet and the exits.
- Mass flow rate (to be minimized)—is the total mass flow of the coolant per unit time.

5. Numerical results

During the optimization process different network branching configurations were automatically developed and tested by the optimization program. Those configurations that produced satisfactory results in terms of the three simultaneous objectives were used to predict a better configuration in the next function evaluation. After each function evaluation, the Pareto front, which is a three-dimensional graph of values of the three objectives as configurations change, moves (Figs. 2–5) until the solution reaches a steady state where no other better solution is feasible, and at this instance optimized points remain in the same configuration without changing. This means that the final shape of the Pareto front is reached and that the optimization process is finished. When the final shape of the Pareto front is reached, the designer can analyze and decide which Pareto optimal point is the best for the desired needs. In this work, choosing the configuration that requires the least amount of pumping power for the coolant was considered to be of great importance.

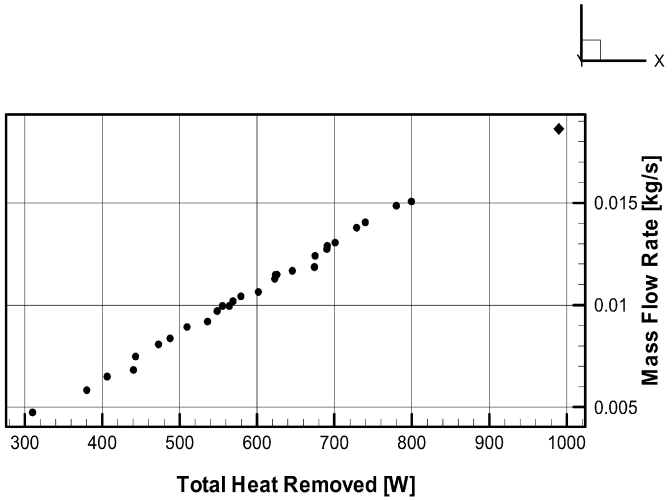

Fig. 2. Pareto optimal points after 1st iteration, $\dot{Q}$–$\dot{m}$ view.

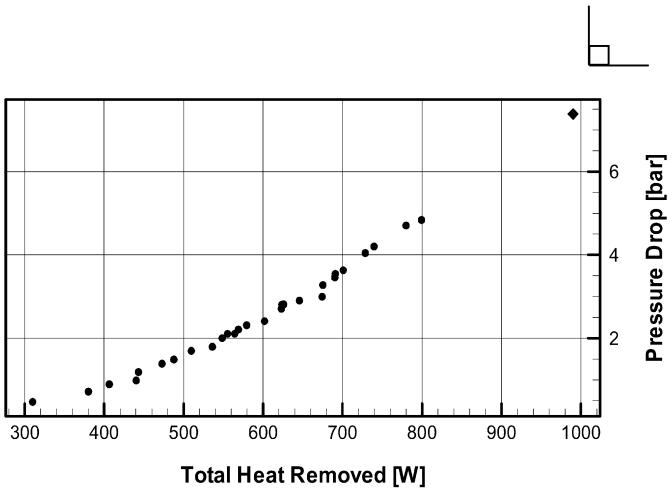

Fig. 3. Pareto optimal points after 1st iteration, $\dot{Q}$–ΔP_t view.

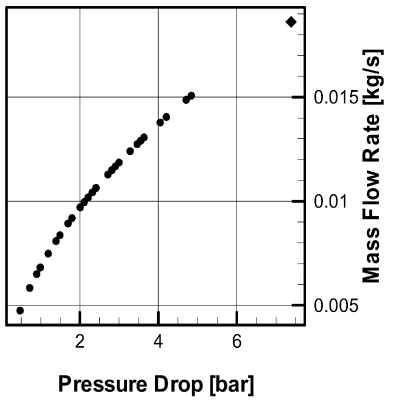

Fig. 4. Pareto optimal points after 1st iteration, ΔP_t–$\dot{m}$ view.

For this particular optimization process there were three objectives, this is why the Pareto front graph is three dimensional. Each axis on the graphs presented in the following figures represents one objective. Each optimal point in the figures that follow has three coordinates. These coordinates are:

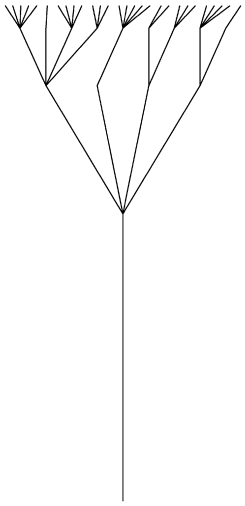

Fig. 5. View of one possible configuration after 1st iteration.

- Total heat removed with units of Watts, plotted in the x-axis.
- Total pressure drop of the coolant with units of bars, plotted in the y-axis.
- Mass flow rate of the coolant with units of kilograms per second, plotted in the z-axis.

In the following figures a two-dimensional view of the Pareto front is presented in order to observe the changes of the three objectives with respect to each other as the optimization process progresses from start to end. These views of the Pareto front show all the optimized points from the particular viewing axis. The diamond shown in the upper right area of all the figures of the Pareto front corresponds to the value of the three objectives for the initial configuration given in Fig. 1. Values of the objectives corresponding to the initial configuration are shown for comparison purposes in Table 1. The optimization process required approximately three hours on a 3.0 GHz Pentium IV processor.

The following results show a sequence of optimized points at various stages in the optimization process. These results are related to the initial configuration shown in Fig. 1 for four branching levels. Figs. 2 through 4 represent optimal designs after the first optimization iteration. Fig. 2 shows the relation between total amount of heat removed and the corresponding coolant mass flow rate. The total heat removed and the coolant mass flow rate are linearly related by the formula

$$\dot{Q} = \dot{m} c_p \Delta T \tag{6}$$

This linear relation is observed in Fig. 2 proving that the optimization algorithm is finding correct cooling network configurations. During the first optimization iteration the optimizer found 28 possible Pareto optimal configurations out of 100, which was the pre-specified number of Pareto points for this optimization case.

Fig. 3 shows the relation between total heat removed and pressure drop. Fig. 4 shows the relation between pressure drop and mass flow rate. Fig. 5 shows one of the possible network

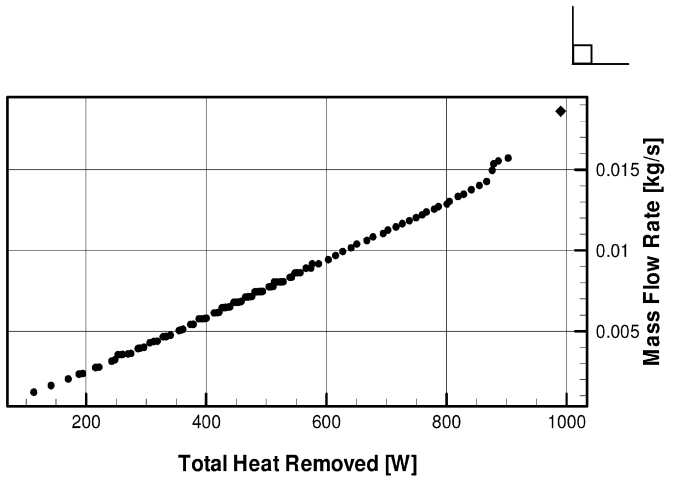

Fig. 6. Pareto optimal points after 500 iterations, $\dot{Q}$–$\dot{m}$ view.

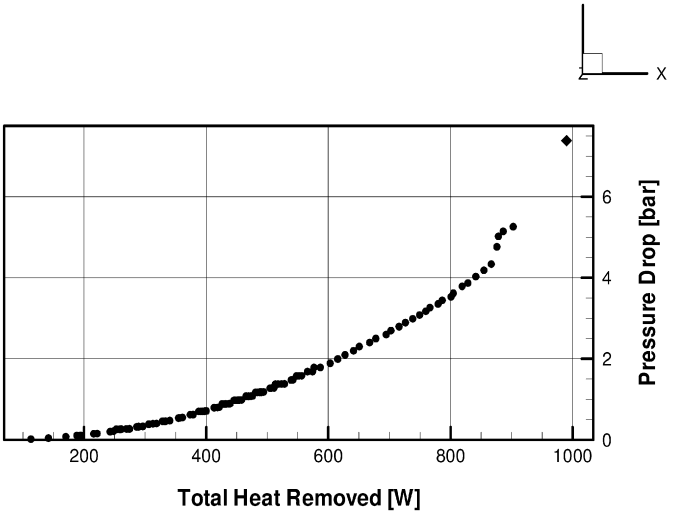

Fig. 7. Pareto optimal points after 500 iterations, $\dot{Q}$–ΔP_t view.

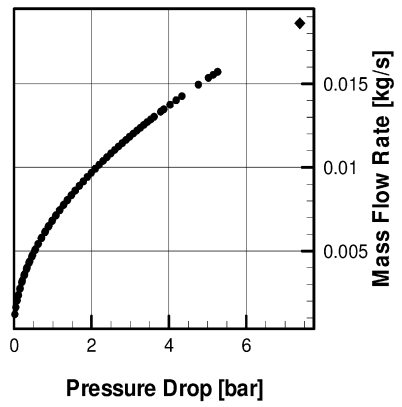

Fig. 8. Pareto optimal points after 500 iterations, ΔP_t–$\dot{m}$ view.

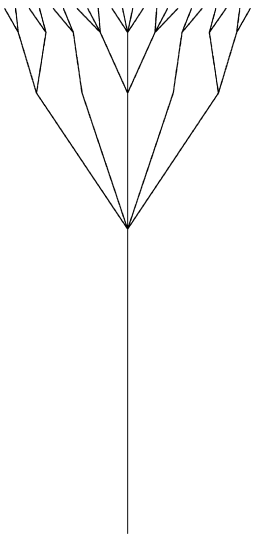

Fig. 9. View of Pareto optimized configuration No. 62 after 500 iterations.

configurations that corresponds to one point on the Pareto front where the heat removed is 548.54 W, the pressure drop is 200.31 kPa, and the mass flow rate is 0.0097044 kg/s.

It should be pointed out that if a linear combination of the single objectives was optimized, it would involve user-specified weighting factors, thus, creating only a single point on the Pareto surface where this point would depend on the chosen weights.

Figs. 6 through 8 represent Pareto optimal front projections after 500 iterations. The optimization was stopped at this stage because there was little change in the shape of the Pareto front. That is, for comparison purposes the number of optimization iterations was increased to 1000 to confirm that the Pareto front was at its most optimized shape. It was noted that very minor changes occurred near the upper-right-hand corners of Figs. 6 through 8. Since the changes in the Pareto front were very concentrated and only in one far extreme it was determined that 500 iterations are a good point to stop the optimization process.

Fig. 6 shows the relationship between the total amount of heat removed and the corresponding required coolant mass flow rate.

Fig. 7 shows the relationship between the total amount of heat removed and the total pressure drop incurred in the coolant network.

Fig. 8 shows the relationship between the total pressure drop and the coolant mass flow rate. Fig. 9 shows one of the possible geometric configurations corresponding to a point No. 62 on the Pareto front consisting of 100 points where the total heat removed is 523.56 W, the total pressure drop is 137.65 kPa, and the coolant mass flow rate is 0.0080506 kg/s. However, there are 100 different optimized configurations to choose from in this test case. These are now the final optimized values of the three objectives and are ready for analysis. This analysis and the criteria for choosing the final optimized design are performed in the next section.

6. Analysis of optimized results

Only those optimum points obtained after 500 iterations were considered. The population was 60 and it was kept con-

Table 2
Performance indicators for a number of optimized cooling networks with four branching levels: a select subset of a hundred Pareto optimal designs after 500 optimization iterations

Pareto point No.	$\dot{Q}$ [W]	ΔP_t [kPa]	$\dot{m}$ [kg/s]	% change in $\dot{Q}$	% change in ΔP_t	% change in $\dot{m}$	Number of branches	Number of exits
Initial	990.02	738.20	0.018614	00.00	00.00	00.00	156	125
1	112.94	1.77	0.0012265	88.59	99.76	93.41	10	3
3	170.18	7.53	0.0020396	82.81	98.98	89.04	12	5
4	188.21	10.67	0.0023470	80.99	98.55	87.39	13	6
6	215.71	15.06	0.0027464	78.21	97.96	85.25	14	7
7	221.39	15.40	0.0027751	77.64	97.91	85.09	14	7
10	253.02	25.88	0.0035483	74.44	96.49	80.94	19	9
15	286.47	31.89	0.0039220	71.06	95.68	78.93	21	10
20	318.70	39.94	0.0043835	67.81	94.59	76.45	19	11
25	354.65	53.49	0.0050456	64.18	92.75	72.89	24	13
30	387.83	70.18	0.0057688	60.83	90.49	69.01	28	15
35	412.99	79.35	0.0061287	58.28	89.25	67.07	30	16
40	431.95	88.63	0.0064723	56.37	87.99	65.23	30	17
45	450.44	97.69	0.0067923	54.50	86.77	63.51	31	18
50	473.21	107.97	0.0071364	52.20	85.37	61.66	33	19
51	475.83	108.31	0.0071515	51.94	85.33	61.58	33	19
52	480.84	117.12	0.0074309	51.43	84.13	60.08	34	20
53	483.95	117.33	0.0074370	51.12	84.11	60.05	34	20
54	487.92	117.70	0.0074482	50.72	84.06	59.99	34	20
55	490.24	117.72	0.0074490	50.48	84.05	59.98	34	20
56	493.97	118.06	0.0074630	50.11	84.01	59.91	35	20
57	504.59	127.31	0.0077451	49.03	82.75	58.39	36	21
58	507.02	127.34	0.0077464	48.79	82.75	58.38	36	21
59	511.19	127.93	0.0077668	48.37	82.67	58.27	36	21
60	513.26	137.36	0.0080423	48.16	81.39	56.79	37	22
62	523.56	137.65	0.0080506	47.12	81.35	56.75	37	22
65	542.19	148.10	0.0083514	45.23	79.94	55.13	40	23
70	574.30	168.50	0.0089047	41.99	77.17	52.16	42	25
73	603.22	189.05	0.0094296	39.07	74.39	49.34	43	26
75	627.20	209.60	0.0099268	36.65	71.61	46.67	48	29
80	694.50	259.88	0.0110490	29.85	64.80	40.64	58	36
85	749.35	307.97	0.0120250	24.31	58.28	35.40	62	39
90	800.86	353.04	0.0128730	19.11	52.18	30.84	69	44
95	854.67	418.61	0.0140160	13.67	43.29	24.70	77	52
100	902.62	526.13	0.0157130	8.83	28.73	15.59	96	68

stant. Thus, there were 30 000 network configurations analyzed. The number of Pareto points was specified to be 100; thus, the number of optimal designs obtained from the optimization is 100. In order to choose the best four-level cooling network design among these 100 Pareto optimal designs, the optimized objectives were compared to the calculated values of total heat removed, total pressure drop, and mass flow rate of the initial configuration shown in Fig. 1. These values were taken as reference and are shown in Table 2.

To determine the best design from the data presented in Figs. 6 through 8 it is necessary to plot the ratio of total heat removed to pumping power, $\frac{\dot{Q}\rho_{\text{avg}}}{\Delta P_t \dot{m}}$, as a function of total heat removed, $\dot{Q}$. The best design is the one where the total heat removed to pumping power ratio is the highest among the other designs. This ratio must be the highest because the objective is to remove as much heat as possible with the least amount of pumping power. In Fig. 10 the single diamond symbol represents the ratio of the total heat removed and the pumping power of the initial configuration and the circles represent the same ratios for all the Pareto points in Figs. 6 through 8.

Fig. 11 shows the pumping power necessary to drive the cooling fluid through the network plotted as a function of total heat removed [12,20]. The dotted line in Fig. 11 represents the values that would exist if the pumping power would be equal to the total heat removed, meaning that for one Watt of power needed to drive the flow, one Watt of heat is removed by the coolant. All the points below the dotted line are good solutions, because the power needed to pump the coolant is less than the amount of total heat removed. All the points above the dotted line are the unfavorable solutions, because more power is needed for pumping than the amount of heat removed.

Note that the initial configuration, which is represented by the diamond, falls in the unfavorable region. All the points plotted in Fig. 11 are arranged from left to right in the same ascending order of Pareto points in Figs. 6 through 8. Therefore, the left most point corresponds to Pareto point No. 1 and the right most point corresponds to Pareto point No. 100. This kink that still exists in the Pareto front at the high flow rates and the high amounts of heat removed (Fig. 11) represents a visual measure of the degree to which the Pareto front has converged.

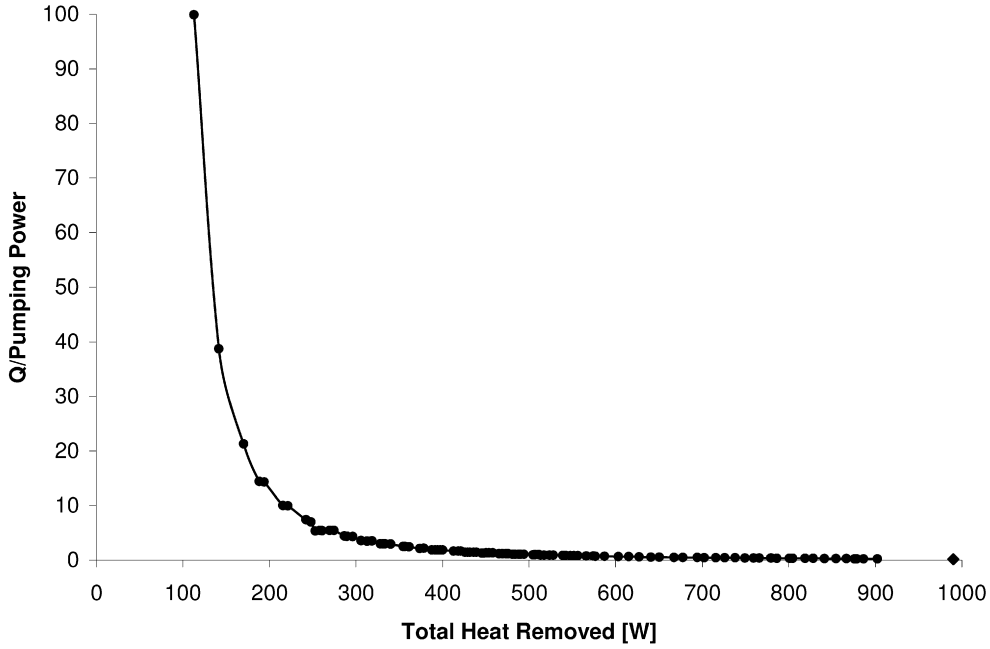

Fig. 10. Ratio of total heat removed-to-pumping power, $\frac{\dot{Q}\rho_{\text{avg}}}{\Delta P_t \dot{m}}$, as a function of total heat removed, $\dot{Q}$.

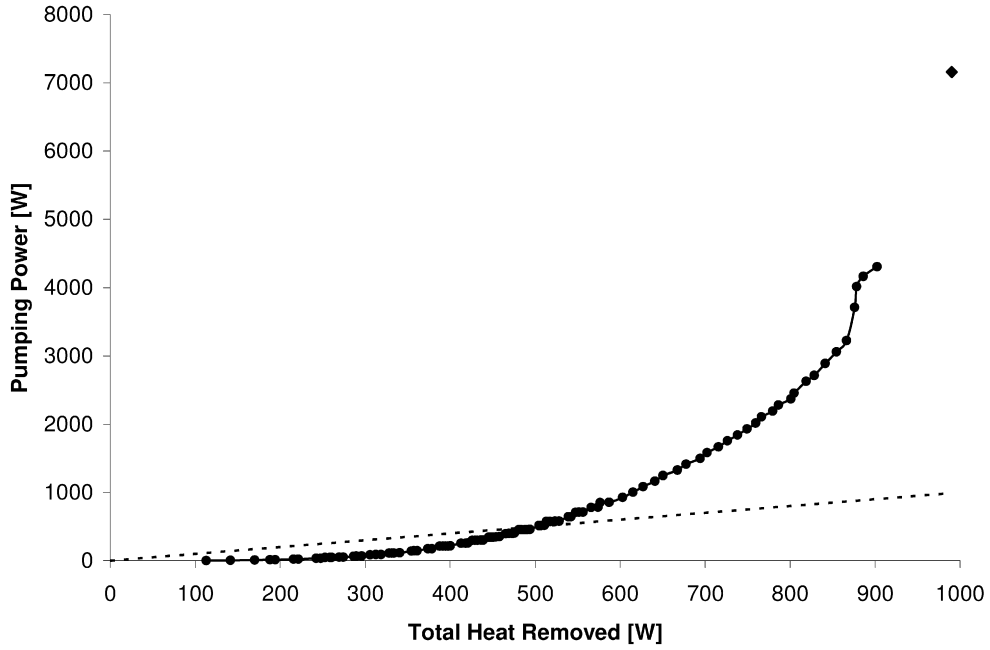

Fig. 11. Cooling efficiency depiction: required pumping power, $\frac{\dot{m}\Delta P_t}{\rho_{\text{avg}}}$, versus total heat removed, $\dot{Q}$.

After using more than twice of the otherwise quite sufficient number of optimization iterations (in this test case it was 500 iterations), this kink becomes barely noticeable. However, the rest of the Pareto front has not moved any more during this significantly longer iterative process. Therefore, for all practical purposes the Pareto front, even with this small local kink, can be considered as converged.

Fig. 12 below is a magnification of the favorable region of Fig. 11, which consists of all the values of pumping power vs. total heat removed under the dashed line. In Fig. 12, all the Pareto points from No. 1 through No. 56 are represented starting with the value of pumping power vs. total heat removed for Pareto point No. 1 at the left most point and concluding with the value of pumping power vs. total heat removed for Pareto point No. 56 at the right most point.

The optimization objectives were to simultaneously maximize the total heat removed, minimize the total pressure drop, and minimize the mass flow rate.

Now, the focus is to select from Fig. 10 the point with maximum ratio of the total heat removed to pumping power. The

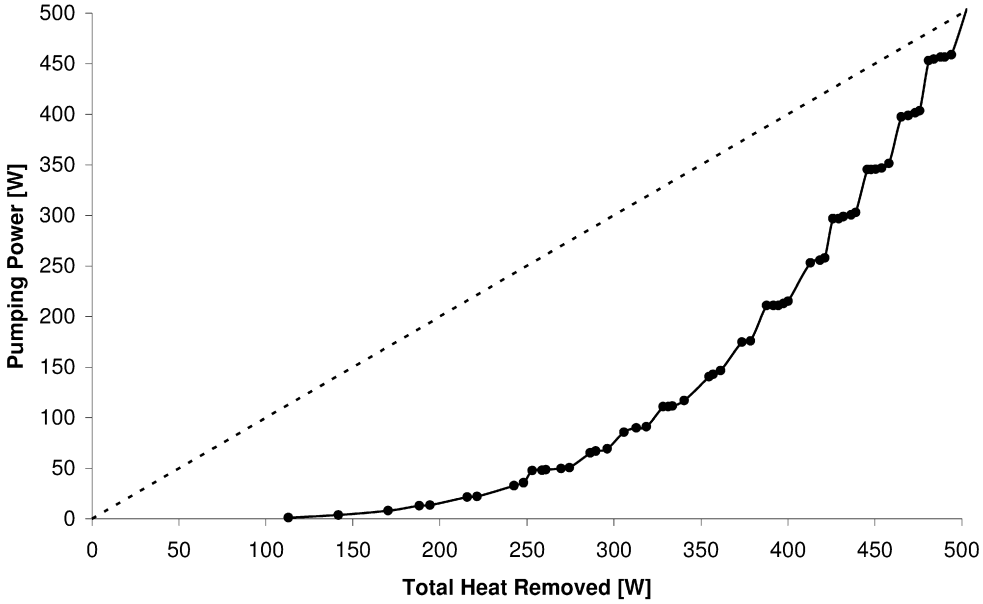

Fig. 12. Magnification of a section of Fig. 11.

point with the highest ratio is beneficial because it is desired to remove the maximum amount of heat while minimizing the total pressure drop; also it is desired to remove the maximum amount of heat while minimizing the pumping power required to circulate the coolant fluid. From Fig. 10 the point with the highest total heat removed to pumping power ratio corresponds to Pareto optimized network No. 1. However, Pareto point No. 1 provides the smallest total heat removed, smallest total pressure drop, and smallest mass flow rate. Consequently, this point also has the best total heat removed to pressure drop ratio and the best total heat removed to pumping power ratio. Greater detail of the amount of pumping power necessary to move the coolant flow and the amount of total heat removed for the configuration of Pareto point 1 is observed in Fig. 12. On such domains one can follow the "evolution" of the configuration toward better and better, in time. This mental viewing is part of the constructal theory today and is acknowledged as such.

The values of total heat removed, $\dot{Q}$, coolant total pressure drop, ΔP_t, and coolant mass flow rate, $\dot{m}$, at Pareto optimized network No. 1 are 112.94 W, 0.0177 bars, and 0.0012265 kg/s, respectively. Fig. 13 is the geometric configuration of the fractal branching channel network associated with Pareto point No. 1. This figure shows the branches orientation only, parameters like the cross-sectional area, hydraulic diameter, and branching level lengths remained fixed for each branching level as described in Table 1. In Fig. 13, the first branching level which is the inlet, has one channel, while the second, third and fourth branching levels have three channels per level. This configuration is the easiest among the other possible configurations to manufacture with only ten branching channels, one inlet, and three exits. It could be expected that this cooling network configuration also provides less fouling of the branching channels.

The optimized results could be viewed from another angle by taking into consideration that at the present time it is expected from a cooling network to remove approximately

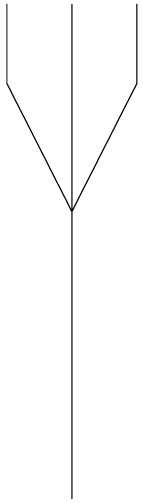

Fig. 13. Geometry of Pareto optimal network No. 1 after 500 iterations with 4 branching levels.

10 Watts per squared centimeters. Configuration of Pareto optimized network No. 4 provides similar results to those expected. Since the surface area of the object where this particular fractal branching network can be implemented is 18 cm^2, 3 cm wide by 6 cm long, it is expected that this network removes approximately 180 Watts of heat. The configuration of Pareto point number 4 provides a similar amount of total heat removed with 188.21 Watts. This configuration is presented in Fig. 14.

Thus, the configuration of Pareto point No. 4, represented in Figs. 10, 11, and 12 as the fourth point from left to right, provides approximately 14 times total heat removed per each Watt of pumping power necessary. Fig. 12 further enhances this observation by noticing that for the fourth point from left to right the amount of pumping power necessary is approximately 13 Watts and the amount of total heat removed is approximately 188 Watts.

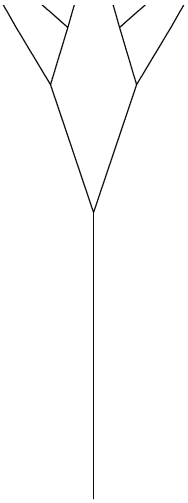

Fig. 14. Geometry of Pareto optimal network No. 4 after 500 iterations with 4 branching levels.

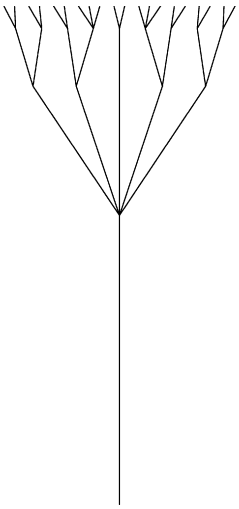

Fig. 15. Geometry of Pareto optimal network No. 56 after 500 iterations with 4 branching levels.

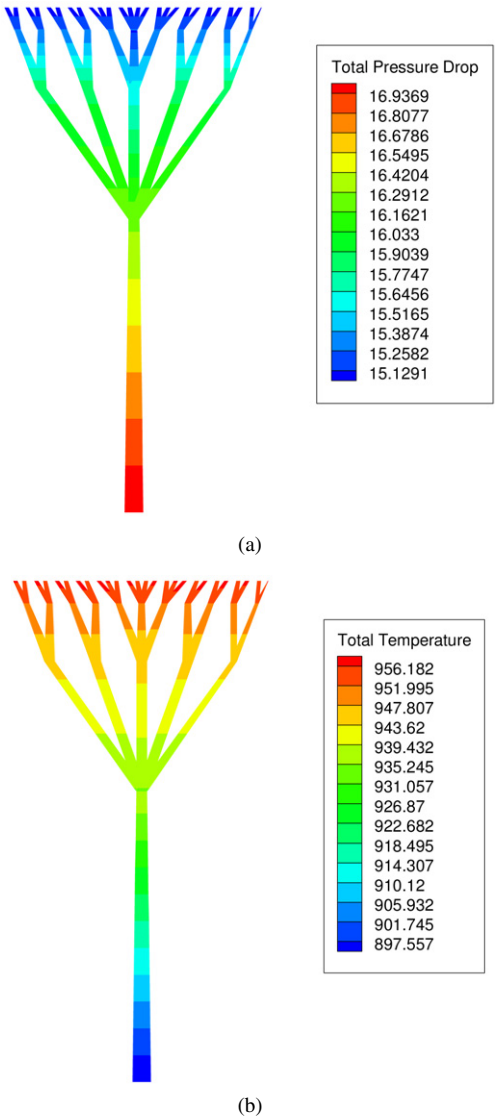

Fig. 16. Geometry of Pareto optimal network No. 73 after 500 iterations with 4 branching levels showing (a) optimized total pressure distribution, and (b) optimized total temperature distribution.

Of particular interest is the optimal design of Pareto point No. 56 for which the amount of thermal energy removed equals the amount of energy spent on facilitating this removal. For optimum design No. 56 the amount of thermal energy removed is 494 Watts, which is approximately half of the maximum possible, 990 Watts for the initial configuration, while requiring only 16% of the original total pressure drop and only 40% of the original mass flow rate. Topology of the branching channels for the optimized design No. 56 is depicted in Fig. 15.

An even more appropriate compromise for the finalist optimized network solution could be the Pareto optimal network number No. 73 (see Table 2). It requires only half of the coolant mass flow rate compared to the initial network configuration given in Fig. 1. It also requires three quarters less pumping power as compared to this initial configuration, while removing 39 percent less heat than the initial configuration with only 43 branches as compared to the original 156 branches. Configuration of the Pareto optimal network No. 73 indicating distribution of corresponding total pressure, total temperature, local mass flow rate and Mach number are given in Figs. 16 and 17.

7. Conclusions

A methodology for preliminary design optimization, of fractal branching channel networks of internal cooling passages utilizing a compressible homo-compositional fluid, has been described and demonstrated. A complete software package was developed for affordable preliminary design optimization of fractal branching channel networks of cooling passages with multiple simultaneous objectives. The software package includes: a random branches generator, a hybrid multi-objective optimizer, a quasi 1-D compressible thermo-fluid analysis code, program OBJ, analyzer and a program to visualize the geometry of the branches.

The only design variables were the number of channels emanating from each of the candidate branching points on each

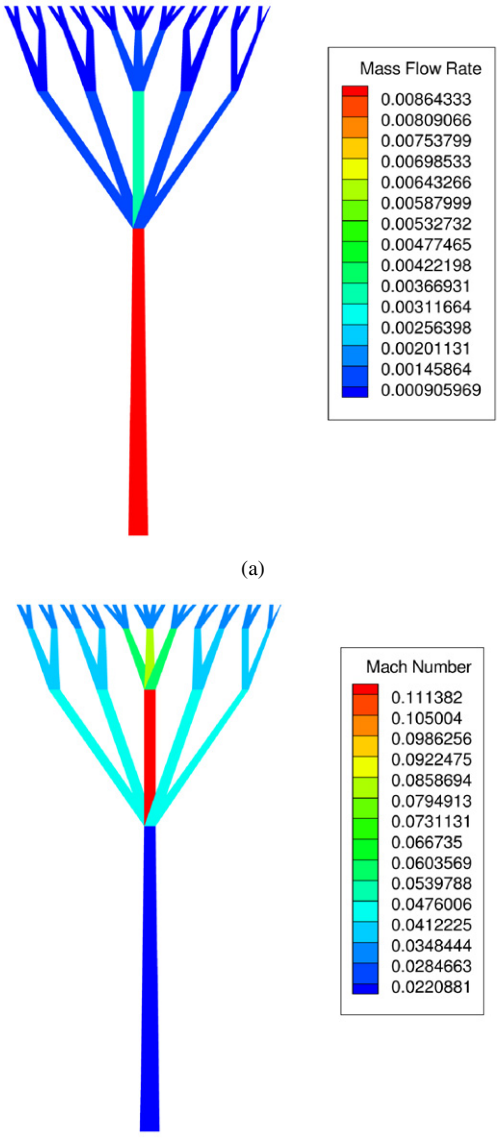

Fig. 17. Geometry of Pareto optimal network No. 73 after 500 iterations with 4 branching levels showing (a) optimized coolant mass flow rate distribution, and (b) optimized Mach number distribution.

of the three levels of branching. Diameters and lengths of the channels on each level of branching were predetermined using the ratio formulas and kept fixed. Surface roughness was specified and kept fixed. No mathematical formulations from the constructal theory [ref] were used in the present work. It serves purely as proof of an alternative concept for designing cooling networks having often-conflicting multiple simultaneous objectives by using a multi-objective optimization algorithm.

In this work the total number of desired optimized cooling network options was specified as one hundred Pareto points. The choice of the single best topology among these 100 optimized cooling networks is then performed depending on the appropriate decision criteria such as the ratio of the total amount of heat removed to total pressure drop ratio from inlet to exit in a cooling network and ratio of the total amount of heat removed to pumping power. These cooling network performance parameters could be further improved using the multi-objective optimization by incorporating each channels' hydraulic diameter, cross-sectional area, length, and wall roughness as additional optimization variables and by adding more branching levels.

The quasi 1-D thermo-fluid analysis code needed approximately forty iterations on average to analyze each configuration. The number of iterations necessary for each network geometry depended on the number of branches per configuration. The hybrid multi-objective optimizer needed 500 iterations to create a converged Pareto front of optimized branching network configurations for the case of four branching levels. A population of 60 designs was used. The total number of function evaluations analyzed was 30 000. The entire design optimization process takes approximately three hours on a single 3.0 GHz Pentium IV processor.

References

[1] M.J. Gonzalez, R.J. Moral, T.J.M. Martin, D. Sahoo, G.S. Dulikravich, N. Jelisavcic, Multi-objective design optimization of topology and performance of branching networks of cooling passages, ASME paper ICNMM2006-96151, in: S. Kandlikar (Ed.), ASME Fourth International Conference on Nanochannels, Microchannels and Minichannels, University of Limerick, Limerick, Ireland, June 19–21, 2006.

[2] T.J. Martin, Computer-automated multi-disciplinary analysis and design optimization of internally cooled turbine blades, Ph.D. dissertation, Department of Aerospace Engineering, The Pennsylvania State University, University Park, PA, 2001.

[3] T.J. Martin, G.S. Dulikravich, Aero-thermo-elastic inverse design and optimization of internally cooled turbine blades, in: M.H. Aliabadi, A.J. Kassab (Eds.), Coupled Field Problems, in: Series on Advances in Boundary Elements, WIT Press, Boston, MA, 2001, pp. 137–184 (Chapter 5).

[4] T.J. Martin, G.S. Dulikravich, Analysis and multi-disciplinary optimization of internal coolant networks in turbine blades, AIAA Journal of Propulsion and Power 18 (4) (2002) 896–906.

[5] G.B. West, J.H. Brown, B.J. Enquist, A general model for the origin of allometric scaling laws in biology, Science 276 (1997) 122–126.

[6] A.Y. Alharbi, D.V. Pence, R.N. Cullion, Temperature distributions in microscale fractal-like branching channel networks, ASME paper HT2003-47501, ASME Summer Heat Transfer Conference, Las Vegas, NV, July 21–23, 2003.

[7] G.S. Dulikravich, R. Moral, D. Sahoo, A multi-objective evolutionary hybrid optimizer, in: R. Schilling, W. Haase, J. Periaux, H. Baier, G. Bugeda (Eds.), EUROGEN 05—Evolutionary and Deterministic Methods for Design, Optimization and Control with Applications to Industrial and Societal Problems, Munich, Germany, September 12–14, 2005.

[8] A. Iorio, X. Li, Solving rotated multi-objective optimization problems using differential evolution, in: Proceeding of the 17th Joint Australian Conference on Artificial Intelligence, Cairns, Australia, 2004.

[9] E. Zitzler, L. Thiele, Multiobjective evolutionary algorithms: A comparative case study and the strength Pareto approach, IEEE Transactions on Evolutionary Computation 3 (4) (1999) 257–271.

[10] R. Eberhart, Y. Shi, J. Kennedy, Swarm Intelligence, Morgan Kaufmann Publ., San Francisco, CA, 2001.

[11] K. Deb, Multi-Objective Optimization using Evolutionary Algorithms, John Wiley & Sons, Baffins Lane, Chichester, England, 2002.

[12] N. Jelisavcic, T.J. Martin, R.J. Moral, D. Sahoo, G.S. Dulikravich, M. Gonzalez, Design optimization of networks of cooling passages, ASME paper IMECE2005-17195, Orlando, FL, November 5–11, 2005.

[13] J.P. Holman, Heat Transfer, fifth ed., McGraw–Hill Book Company, 1981.

[14] S.E. Haaland, Simple and explicit formulas for the friction factor in turbulent pipe flow, ASME Journal of Fluids Engineering 105 (1983) 89–90.
[15] R.W. Barber, D.R. Emerson, Optimal design of microfluidic networks using biologically inspired principles, Microfluidics and Nanofluidics, Research Paper, https://commerce.metapress.com/content/w176523127185244/resource-secured/?target=fulltext.pdf&sid=5vbwsymi2n5fr5aqupm3nj55&sh=www.springerlink.com, 2007.
[16] A. Bejan, Constructal-theory network of conducting paths for cooling a heat generating volume, International Journal of Heat and Mass Transfer 40 (1997) 799–816.
[17] A. Bejan, Shape and Structure, from Engineering to Nature, Cambridge University Press, Cambridge, UK, 2000.
[18] A. Bejan, S. Lorente, Constructal theory of generation of configuration in nature and engineering, Applied Physics Reviews, Journal of Applied Physics 100 (2006) 041301.
[19] X.-H. Ding, K. Yamazaki, Constructal design of cooling channel in heat transfer system by utilizing optimality of branch systems in nature, ASME Journal of Heat Transfer 129 (2007) 245–255.
[20] L. Gosselin, A. Bejan, Tree networks for minimal pumping power, International Journal of Thermal Sciences 4 (2005) 53–63.